Critical dynamics of an interacting magnetic nanoparticle system



2002 J. Phys.: Condens. Matter 14 4901

(http://iopscience.iop.org/0953-8984/14/19/314)

INSTITUTE OF PHYSICS PUBLISHING JOURNAL OF PHYSICS: CONDENSED MATTER

J. Phys.: Condens. Matter **14** (2002) 4901–4914 PII: S0953-8984(02)30073-0

# Critical dynamics of an interacting magnetic nanoparticle system

**M F Hansen[1,2], P E Jönsson[1], P Nordblad[1] and P Svedlindh[1]**

[1] Department of Materials Science, Uppsala University, Box 534, SE-751 21 Uppsala, Sweden
[2] Department of Physics, Building 307, Technical University of Denmark, DK-2800 Kgs. Lyngby, Denmark

Received 24 October 2001, in final form 17 January 2002
Published 2 May 2002
Online at stacks.iop.org/JPhysCM/14/4901

**Abstract**

Effects of dipole–dipole interactions on the magnetic relaxation have been investigated for three Fe–C nanoparticle samples with volume concentrations of 0.06, 5 and 17 vol%. While both the 5 and 17 vol% samples exhibit collective behaviour due to dipolar interactions, only the 17 vol% sample displays critical behaviour close to its transition temperature. The behaviour of the 5 vol% sample can be attributed to a mixture of collective and single-particle dynamics.

## 1. Introduction

The dynamics of systems of interacting ferromagnetic nanoparticles has been the focus of extensive research in recent years. A question of considerable controversy has been the existence of a phase transition to a low-temperature spin-glass-like phase [1–9]. Recent studies on strongly interacting systems have reported a critical slowing down [4, 5, 9] and a critical divergence of the non-linear susceptibility [6]. In addition, non-equilibrium properties such as ageing, memory and rejuvenation phenomena have been observed in magnetic relaxation and low-frequency AC susceptibility measurements at low temperatures [7,10]. These observations indicate the existence of a low-temperature spin-glass-like state. However, some questions about the collective state of interacting nanoparticles are still not resolved. In a recent experimental study of an interacting maghemite nanoparticle system [11], it was not possible to find evidence of a finite-temperature transition to a spin-glass-like phase. Still, the particle system exhibited non-equilibrium dynamics in magnetic relaxation experiments, typical of spin glasses. The absence of a critical behaviour was in this study linked to mixing of collective and single-particle relaxation effects. Mixing of this kind can for instance originate from a broad particle size distribution, or it may be observed in a system with a small volume fraction of particles and therefore comparably weak inter-particle interactions.

In this work, extensive studies of the magnetic dynamics in a close-to-monodisperse nanoparticle system are presented. Three samples having different volume concentrations of nanoparticles were investigated: one dilute and nominally non-interacting sample and two

  

more concentrated interacting samples. Both interacting samples exhibit collective behaviour due to dipolar interactions at low temperatures, but only the most interacting sample displays critical dynamics in the time window investigated and shows equilibrium dynamics quite similar to that of an atomic spin glass.

## 2. Experimental details

The particles were prepared by thermal decomposition of $Fe(CO)_5$ (20.0 ml) in a mixture of carrier liquid (50.0 ml *cis–trans*-decalin) and surfactant (4.0 g oleic acid) by the method described in [12]. This method leads to the formation of surfactant-coated particles of the amorphous alloy $Fe_xC_{1-x}$ ($x \approx 0.2$–$0.3$). The decomposition was carried out slowly by using low heating powers. Great care was taken at all times to avoid oxidation of the particles and a flow of $Ar/H_2$ (98/2%) gas through the reaction vessel was maintained throughout the preparation. After preparation, the decalin carrier liquid was evaporated at 140 °C under reduced pressure using a gas flow to drive out the vapour and a small amount of de-gassed xylene was added such that the volume fraction of particles in the resulting base ferrofluid was about 5 vol%. More dilute samples were obtained by further dilution of this ferrofluid by addition of xylene and more concentrated samples were obtained by evaporating the xylene at room temperature in vacuum. All sample handling after the preparation of the base ferrofluid was carried out in an argon glove box. The chemical state of the iron in the ferrofluids was checked by Mössbauer spectroscopy, which showed that no significant oxidation of the particles had taken place during the sample preparation and sample handling. The particle volume fractions in the resulting samples were estimated from the iron content determined by atomic absorption spectroscopy. The sizes of the particles were determined from transmission electron microscopy (TEM) studies. A droplet of a dilute ferrofluid was placed onto a grid that was left in air for about a week to ensure full oxidation of the particles. The size determination from the resulting TEM micrographs was subsequently corrected for the change in density due to the oxidation of the particles. The shape of the particles was spherical to a good approximation. The particle size distribution was obtained using the computer analysis method described in [13]. The analysis of 1579 particles yielded the average particle diameter $d = 5.3$ nm with the standard deviation 0.3 nm. The volume-weighted volume distribution was well described by the log-normal distribution, $f(V)\,\mathrm{d}V = (2\pi)^{-1/2}(\sigma V)^{-1}\exp[-\ln^2(V/V_m)/2\sigma^2]\,\mathrm{d}V$, with $V_m = 78.2$ nm$^3$ and $\sigma = 0.13$. The present preparation batch is slightly different from that studied previously in [4, 6, 14]. We have studied three samples with particle volume fractions $\phi$ of $17 \pm 4$, $5 \pm 1$ and $0.06 \pm 0.02$ vol%. In the most concentrated sample, most of the carrier liquid was evaporated and the sample had a paste-like consistency. This resulted in poor thermal contact between the sample and the sample container. Thermal stability was not achieved until several minutes after a change in temperature, preventing systematic studies of the non-equilibrium dynamics for this sample.

Two experimental set-ups were used for the magnetic studies. A commercial susceptometer (LakeShore model 7225) was used for DC field scans and AC susceptibility measurements in a frequency range of 15–1000 Hz. A non-commercial superconducting quantum interference device (SQUID) magnetometer [15] was used for AC susceptibility measurements in a frequency range of 10 mHz–9.1 kHz, zero-field-cooled (ZFC) relaxation measurements and magnetic noise measurements. The applied AC and DC fields were chosen small enough (0.1 Oe) to ensure linear response from the samples. The background field was $<1$ mOe. The ZFC relaxation measurements were carried out by cooling the sample to the measuring temperature $T$ in zero field, equilibrating the system for a wait time $t_w$ and then applying a small DC field $h$ and measuring the magnetization $M(T, t)$ as a function of time, $t$,

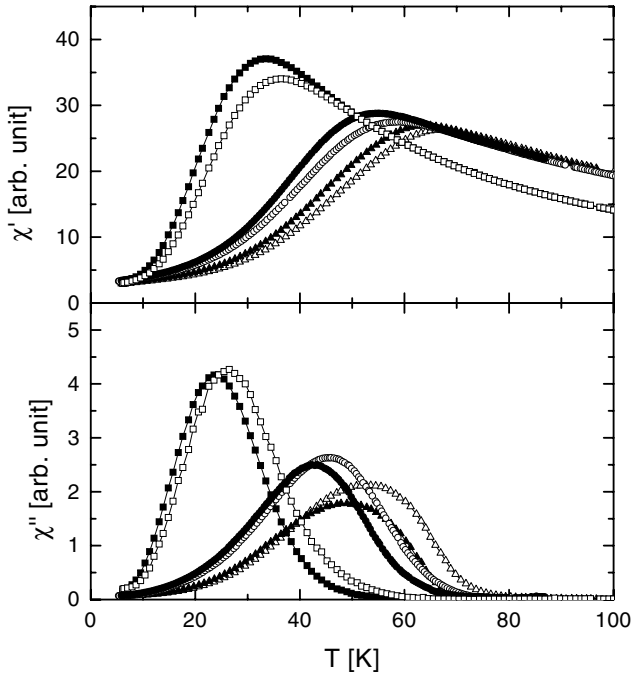


**Figure 1.** AC susceptibilities for the 0.06 vol% (□), 5 vol% (○) and 17 vol% (△) samples at frequencies of $f = 125$ Hz (filled symbols) and $f = 1000$ Hz (open symbols).

after that the field was applied. For a slowly relaxing system, it can be shown that $M(T, t)$ and the relaxation rate $S(T, t) \equiv h^{-1}\partial M(T, t)/\partial \ln t$ relate to the real and imaginary components of the AC susceptibility as [16]

$$M(T, t)/h \approx \chi'(T, \omega), \tag{1}$$

$$S(T, t) \approx \frac{2}{\pi}\chi''(T, \omega), \tag{2}$$

with $t = 1/\omega$. Magnetic noise measurements were performed in zero external field using an HP35670A dynamic signal analyser. The power spectrum of the magnetic fluctuations was measured in three overlapping frequency intervals (i) 0.003–12.5 Hz, (ii) 0.25–400 Hz and (iii) 8–12 500 Hz. The background spectra were subtracted from the data. Data of the same order of magnitude as the background signal were not used in the analysis. The fluctuation-dissipation theorem [17] relates the noise power spectrum to the zero-field limit of the out-of-phase AC susceptibility as

$$P(T, \omega) = 4k_B T \frac{\chi''(T, \omega)}{\omega}. \tag{3}$$

A comparison between the out-of-phase component obtained from AC susceptibility measurements and results obtained from zero-field noise measurements verifies that equation (3) is obeyed and hence that the AC data are obtained in the linear response regime.

## 3. Results and discussion

### *3.1. General behaviour*

Figure 1 shows the AC susceptibility measured in the commercial set-up for the three samples. The most dilute sample with a 0.06 vol% fraction of particles is intended to serve as an

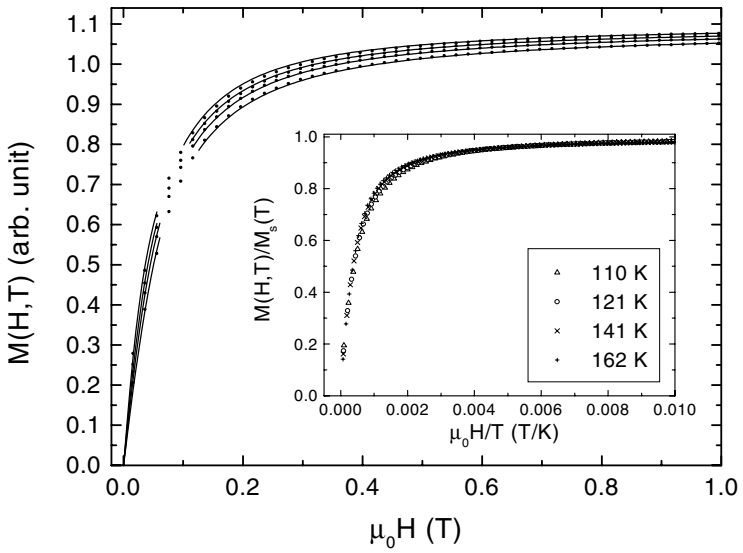


**Figure 2.** Magnetization versus field measured for the 5 vol% sample at $T = 110$, 121, 141 and 162 K (top to bottom). The curves are the fits described in the text. The inset shows the magnetization normalized to saturation versus $H/T$.

experimental reference for a non-interacting system. However, the peak height of $\chi''$ for this sample increases slightly with increasing frequency. This trend is opposite to the expected behaviour for non-interacting nanoparticles [18] and thus indicates that the dynamics of this sample is influenced by weak inter-particle interactions. Despite this, it is possible to assess the distribution of energy barriers with reasonable accuracy making use of the method described in [19]. This analysis yields the pre-exponential factor $\tau_0 = 1 \times 10^{-12}$ s and anisotropy constant $K = 0.9 \times 10^5$ J m$^{-3}$ in the Arrhenius–Néel expression

$$\tau = \tau_0 \exp\left(\frac{KV}{k_B T}\right). \tag{4}$$

The extracted values of $K$ and $\tau_0$ compare reasonably well with previous estimates. For 5.0 nm Fe–C particles, $K$ has been estimated to $1.3 \times 10^5$ J m$^{-3}$, and it has been found that $K$ increases with decreasing particle size to $3 \times 10^5$ J m$^{-3}$ for 3.2 nm particles [20, 21]. Studies of batches with different preparation routes have reported values of $\tau_0$ in the range $2 \times 10^{-12}$–$3 \times 10^{-11}$ s [4, 14, 21, 22].

To estimate the saturation magnetization, $M_s(T)$, of the particles we use $m$ versus $H$ curves measured on the 5 vol% sample at $T = 110$, 121, 141 and 162 K (see figure 2). Although these temperatures are well above the superparamagnetic blocking temperature of the particles, the magnetization curves are not expected to follow the well-known Langevin function for non-interacting isotropic superparamagnets, unless the anisotropy energy and dipolar interaction energy are negligible compared to the thermal energy, i.e., $\sigma = KV/(k_B T) \ll 1$ and $\xi_D = \mu_0 M_s^2 V\phi/(4\pi k_B T) \ll 1$, where $M_s$ denotes the saturation magnetization. For the measurements performed here, $\sigma \sim 3$–5 and the anisotropy has therefore to be included in the analysis. We initially assume that the dipolar energy is negligible and analyse the magnetization curves in terms of the results of [23] for non-interacting anisotropic particle systems using the approximations for the low- and high-anisotropy limits given in section III.C.3 of that paper. The solid curves in figure 2 correspond to these fits, and the gaps in the lines are the transition

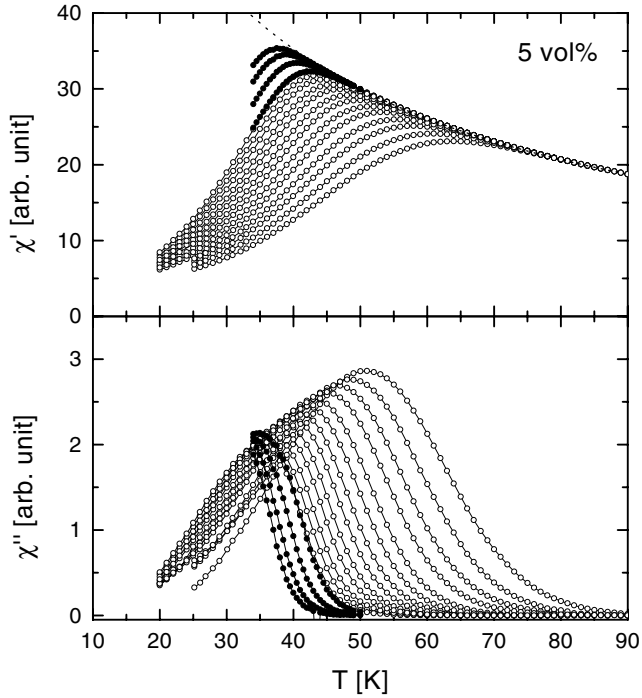


**Figure 3.** AC susceptibilities for the 5 vol% sample using the frequencies (left to right, open symbols) $f = 0.010$, 0.031, 0.091, 0.31, 0.91, 3.1, 9.1, 31, 91, 310, 910, 3100, 9100 Hz. The filled points are obtained from ZFC relaxation measurements and correspond to the frequencies $f = 0.019$, 0.103, 0.979, 10.1 mHz. The dashed curve indicates the equilibrium susceptibility.

regions between the two approximations. Using the anisotropy constant and particle volume determined above, the saturation magnetization was derived from these fits. The temperature dependence of $M_s$ was well described by the relation $M_s(T) = M_s(0)(1 - aT^b)$ with $a = 2 \times 10^{-6}[\mathrm{K}^{-b}]$ and $b = 1.9$ (compare with [22]) and we find $M_s(0) = 9.6 \times 10^5$ A m$^{-1}$. It is now possible to estimate that $\xi_D \sim 0.2$ for the temperature range used here, which validates the neglect of the dipolar term in our analysis. The importance of including the anisotropy in the analyses of the magnetization curves is further illustrated in the inset of figure 2 in the plot of $M(H, T)/M_s(T)$ versus $H/T$ where deviations from the data collapse expected for a Langevin function are clearly seen near $\mu_0 H/T = 0.002$ T/K for the lowest temperatures.

Figures 3 and 4 show the AC susceptibility data measured in the non-commercial SQUID for the 5 and 17 vol% samples, respectively. For the 5 vol% sample, ZFC relaxation data are also included. A few differences in the behaviour of these samples as compared to the dilute sample can immediately be noticed. The peak height of $\chi''$ increases significantly with increasing frequency, and the width of the peak increases with increasing frequency. The onset of a non-zero $\chi''$, is shifted towards higher temperatures and it becomes sharper with increasing volume fraction of particles.

Figure 5 shows the relaxation rate for the 5 vol% sample measured for two different wait times at different temperatures. Below 40 K, a clear wait time dependence is observed, indicating that non-equilibrium phenomena play a key role for the dynamics at low temperatures. The same sample has recently been subject to a detailed study of the low-temperature non-equilibrium dynamics in which the memory effect in the AC susceptibility was

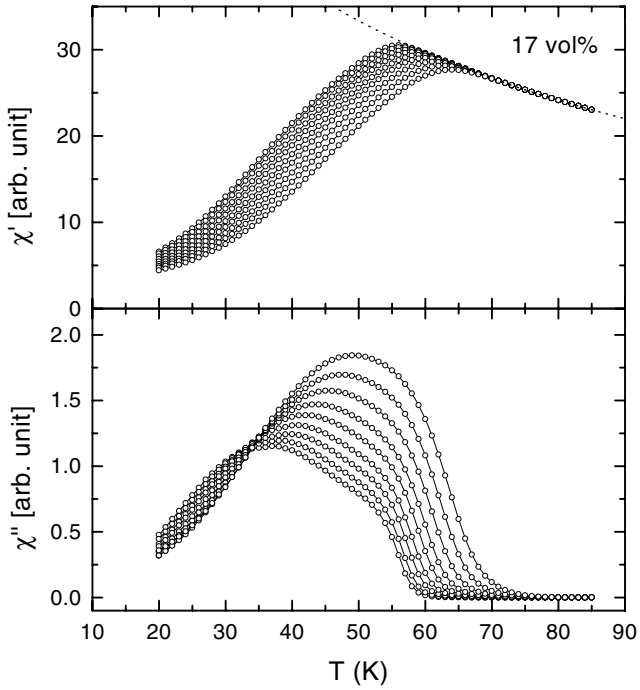


**Figure 4.** AC susceptibilities for the 17 vol% sample using the frequencies (left to right) $f = 0.017$, 0.051, 0.17, 0.51, 1.7, 5.1, 17, 51, 170 Hz. The dashed curve indicates the equilibrium susceptibility.

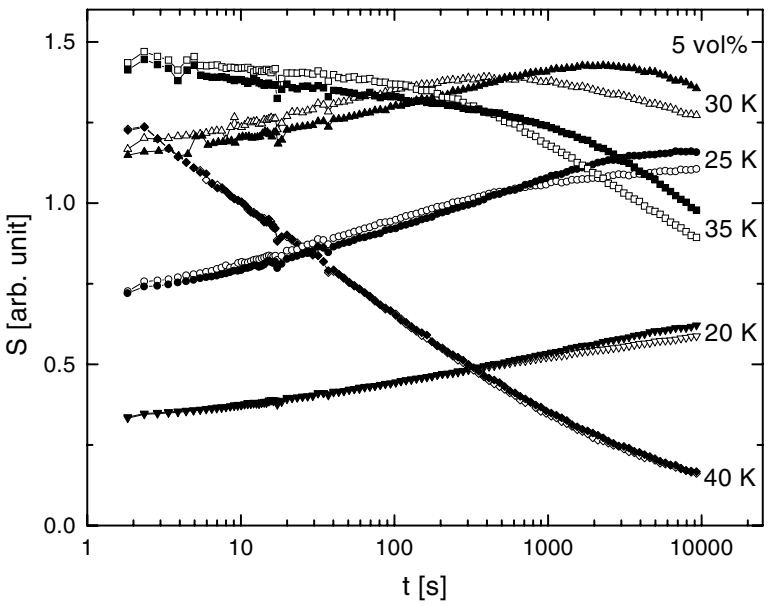


**Figure 5.** Relaxation rate for the 5 vol% sample obtained from ZFC relaxation measurements at the temperatures indicated after wait times of 300 s (open symbols) and 3000 s (filled symbols).

observed and further characterized by temperature-cycling ZFC relaxation experiments [10]. It was shown that the non-equilibrium dynamics in this sample is governed by long-range collective behaviour and that well-known concepts for spin glasses such as memory and rejuvenation are necessary to describe the observations. This implies that the magnetic relaxation of the two concentrated samples must be analysed in terms of collective dynamics. A model for weakly interacting particles, such as that proposed in [24], where the effect of dipolar interaction on the relaxation time is accounted for by introducing the thermodynamic averages of the local dipolar field in a rigorous expression for the single-particle relaxation time, is only valid at temperatures much higher than the freezing temperatures of the two concentrated samples. Below, we briefly introduce the concepts of dynamic scaling and discuss the observed dynamics for the two concentrated samples in terms of critical dynamics.

### *3.2. Dynamic scaling*

A signature of a continuous magnetic phase transition is the divergence of the correlation length, $\xi$, when the phase transition temperature, $T_g$, is approached from above as $\xi/a = \epsilon^{-\nu}$, where $a$ is the average distance between interacting moments, $\epsilon = T/T_g - 1$ is the reduced temperature and $\nu$ is a critical exponent. According to conventional critical slowing down, the longest relaxation time due to correlated dynamics, $\tau_c$, is related to the correlation length as $\tau_c \propto (\xi/a)^z$, where $z$ is the dynamic critical exponent. Hence, for $T \to T_g^+$

$$\tau_c = \tau_* \epsilon^{-z\nu}, \tag{5}$$

where $\tau_*$ is a microscopic relaxation time. According to the dynamic scaling hypothesis [25], for $T \to T_g^+$ and $t/\tau_* \gg 1$, the spin auto-correlation function can be written in the scaling form [26]

$$q(t) = t^{-\beta/z\nu} Q(t/\tau_c), \tag{6}$$

where $\beta$ is a critical exponent and $Q(x)$ is a scaling function. Using linear response theory it is possible from this relation to obtain the complex susceptibility and derive the scaling relation [27]

$$\frac{\chi''(T,\omega)}{\chi_{eq}(T)} = \epsilon^{\beta} G(\omega\tau_c), \tag{7}$$

where $\omega = 1/t$ and $G(x)$ is a scaling function. The asymptotic behaviour is $G(x) \propto x^y$, with $y = 1$ and $\beta/z\nu$ for small and large values of $x$, respectively. Using the asymptotic behaviour of $G(x)$ in the limit $\omega\tau_c \to 0$, the following relation holds: [26–28]

$$\frac{1}{\omega}\frac{\chi''(T,\omega)}{\chi_{eq}(T)} \propto \epsilon^{-z\nu+\beta} \propto \tau_c^{1-\beta/z\nu}, \tag{8}$$

implying that the left-hand side of equation (8) at each temperature reaches a frequency-independent plateau.

The meaning of $\tau_*$ is that it is the relaxation time of the individual magnetic entities in the system. For spin glasses, $\tau_* \sim 10^{-13}$ s and is the fluctuation time of an atomic moment. For nanoparticles, $\tau_*$ can be assigned to the superparamagnetic relaxation time of a single particle of average size. In a dense system, the dipolar interaction may modify this relaxation time compared to that of isolated particles. However, as a first approximation, it is reasonable to assume that $\tau_*$ is close to the superparamagnetic relaxation time of an isolated particle, which in the relevant temperature range for our studies can be approximated by Arrhenius–Néel expression (equation (4)). Below, we compare two approximations: (i) $\tau_* =$ constant, and (ii) $\tau_* = \tau_0 \exp(KV_m/k_BT)$. The first approximation has been used in previous

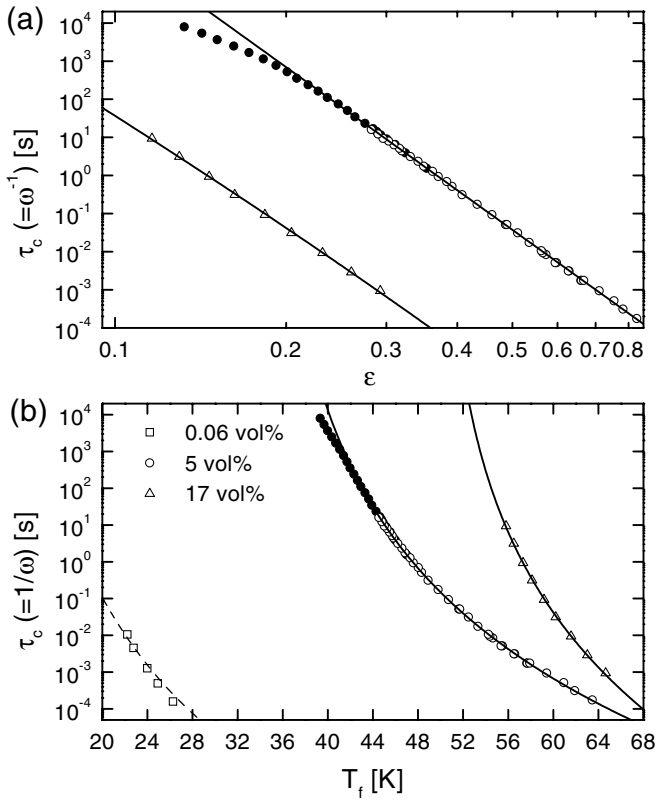


**Figure 6.** (*a*) Relaxation time $\tau_c = \omega^{-1}$ versus reduced temperature for the 5 and 17 vol% samples. Open and filled points are obtained from AC susceptibility and ZFC relaxation measurements, respectively. The curves are fits to equation (5) as described in the text. (*b*) Relaxation time versus temperature for the 0.06, 5 and 17 vol% samples. The freezing temperatures for the 5 and 17 vol% samples were obtained from $\chi'$ as described in the text. For the 0.06 vol% sample, the data correspond to the peak temperatures of $\chi''$, and the Arrhenius–Néel expression with parameter values as given in the text is shown as a dashed curve.

work [4–6, 9, 29], but it is only a good approximation if there is little variation of the single-particle relaxation time in the temperature interval used for the analysis.

In AC susceptibility experiments, the slowing down of the relaxation time $\tau_c$ (equation (5)) can be derived from the temperatures corresponding to the onset of dissipation (freezing temperatures) as a function of the observation time $\omega^{-1}$. We have considered two criteria for the onset. In the first criterion, the freezing temperature is defined as the temperature at which $\chi''(T, \omega)$ attains 15% of its maximum value. In the second criterion, the freezing temperature is defined from the relation $\chi'(T_f, \omega) = 0.98\chi_{eq}(T_f)$. Figure 6(*b*) shows the freezing temperatures for the two concentrated samples obtained from $\chi'$-data. The superparamagnetic blocking temperatures estimated from the peaks of the $\chi''$-data for the dilute sample are included for comparison.

*3.2.1. 17 vol% sample.* First, we consider the approximation $\tau_* =$ constant. Using the out-of-phase susceptibility data, a dynamic scaling analysis according to equation (5) results in $T_g = 49.5 \pm 2$ K, $z\nu = 10.5 \pm 2$ and $\tau_* = 10^{-7.7\pm1}$ s [29]. This analysis is performed

for reduced temperatures in the range $0.16 \lesssim \epsilon \lesssim 0.37$ and corresponds to four decades of observation times. A similar analysis using the in-phase susceptibility data results in $T_g = 50.5 \pm 2$ K, $z\nu = 9.5 \pm 2$ and $\tau_* = 10^{-8.3\pm1}$ s. The values of $T_g$ and $z\nu$ from the two analyses are in good agreement, and the value of $\tau_*$ is, considering the temperature interval used in the analysis and the estimates of $\tau_0$ and $K$ given above, within the limits implied by the Arrhenius–Néel expression. The derived values of $z\nu$ also compare well to values found in previous work on nanoparticles: $z\nu = 11 \pm 3$ in [4] and $10.5 \pm 3$ in [9], but less well to $z\nu = 7.0 \pm 0.3$ found in [5]. A good agreement is also found comparing with canonical three-dimensional Ising and Heisenberg spin glasses, for which $z\nu = 8$–$10$ [27,28]. An analysis according to the full scaling relation, equation (7), using $T_g = 49.5 \pm 1.5$ and $z\nu = 10.5 \pm 2.0$, yields data collapse for $\beta = 1.1 \pm 0.2$ (see [29], figure 3). This analysis is based on all available $\chi''$-data with temperatures corresponding to $\epsilon > 0.01$ ($T > 50$ K). The value of $\beta$ is in good agreement with $\beta = 1.2 \pm 0.1$ obtained from a full scaling analysis of the non-linear magnetic susceptibility on a similar sample [6], but larger than typical values of $\beta = 0.5$–$0.8$ reported for three-dimensional Ising and Heisenberg spin glasses [27,30,31]. The value of $\beta/z\nu \approx 0.11$, extracted from the asymptotic behaviour of $G(x)$ for large $x$, is consistent with the derived values of $\beta$ and $z\nu$.

Next, we consider the effect of using $\tau_* = \tau_0 \exp(KV_m/k_BT)$. It should be noted that this introduces one extra parameter that can be varied in the analysis, and we have therefore explored the critical behaviour for a variety of choices of $\tau_0$ and $KV_m$ to evaluate the robustness of the estimates of $z\nu$ and $\beta$. Critical slowing down analyses have been performed for various fixed values of $\tau_0$ and $T_g$ and the values of $z\nu$ and $KV_m$ have been estimated and used in the analysis according to the scaling relation, equation (7), to extract the value of $\beta$. From these analyses, it is found that both the critical slowing down relation and the full scaling relation can be fulfilled for $T_g = 50 \pm 2$ K with $\tau_0 = 1 \times 10^{-11}$ s. The estimate of $KV_m/k_B$ depends slightly on whether the $\chi'$-data or the $\chi''$-data are used in the critical slowing down analysis, and the corresponding parameter intervals are $KV_m/k_B = 500 \pm 100$ K using $\chi'$ (shown in figure 5) and $KV_m/k_B = 650 \pm 100$ K using $\chi''$. For both analyses, the extracted critical exponents attain the values $z\nu = 8.5 \pm 2$ and $\beta = 0.9 \pm 0.2$. Other values of $\tau_0$ of the order of $10^{-11}$ s yield slightly different values of $KV_m/k_B$ but the same values of the critical exponents. The values of $KV_m/k_B$ and $\tau_0$ are of the same size as the estimates for the dilute sample, $KV_m/k_B \approx 510$ K and $\tau_0 \sim 1 \times 10^{-12}$ s. This is what would be expected if the effect of the inter-particle interactions were accounted for solely by the critical divergence of $\tau$ (equation (5)). The values of $z\nu$ and $\beta$ are slightly smaller than those obtained from the analysis assuming a constant $\tau_*$. The decrease of $z\nu$ is due to the fact that the temperature dependence of $\tau_c/\tau_*$ is weaker when $\tau_*$ is allowed to vary with temperature. The reduced value of $z\nu$ and the extracted smaller value of $\beta$ leads to $\beta/z\nu \approx 0.11$, which is the same value as was found from the analysis using a constant value of $\tau_*$. The data collapse of $\epsilon^{-\beta}\chi''(T)/\chi_{eq}(T)$ versus $\omega\tau_c$ to a single function $G(x)$ according to equations (5) and (7) using $\tau_0 = 10^{-11}$ s and $KV_m/k_B = 570$ K (the average of the values obtained using $\chi'$ and $\chi''$ in the critical slowing down analyses) is shown in figure 7. The scaling is of the same quality as that assuming a constant $\tau_*$, and the asymptotic behaviours are the same (in agreement with the estimates of $\beta$ and $z\nu$).

Figure 8($b$) shows $\chi''(\omega)/\omega\chi_{eq}$ as a function of $\omega$ for different temperatures $T > T_g$ in a log–log plot for the 17 vol% sample. The prediction of plateaus at low frequencies from equation (8) holds regardless of a temperature dependence of $\tau_*$ and figure 8($b$) shows that the prediction is well confirmed for this sample. In the same figure, the behaviour calculated from equation (7) is also included using the experimentally determined scaling function, $G(x)$, and extrapolating using its asymptotic behaviour.

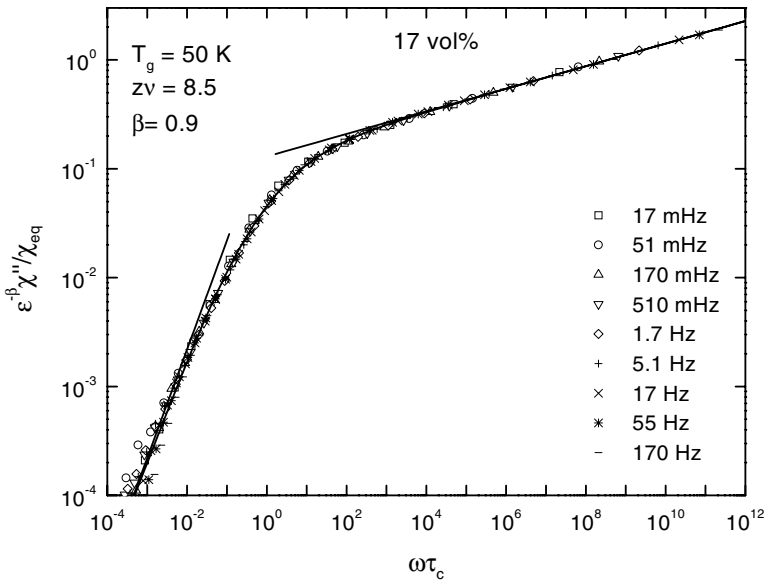


**Figure 7.** The full dynamic scaling plot for the 17 vol% sample according to equation (7) using the Arrhenius–Néel expression for $\tau_*$ as described in the text. The asymptotic behaviours of $G(x)$ are shown as straight lines.

*3.2.2. 5 vol% sample.* For the 5 vol% sample, an apparent scaling according to equation (5) with a constant value of $\tau_*$ can be obtained for temperatures corresponding to $0.25 \lesssim \epsilon \lesssim 0.8$ (six decades of observation times) with $T_g = 35.1 \pm 2$ K, $z\nu = 10.8 \pm 1$ and $\tau_* = 10^{-4.5\pm0.5}$ s using $\chi''$-data, and with $T_g = 34.6 \pm 2$ K, $z\nu = 10.8 \pm 1$ and $\tau_* = 10^{-4.7\pm0.5}$ s using $\chi'$-data and ZFC relaxation data (shown in figure 6). However, deviations from scaling are found at lower temperatures ($\epsilon < 0.25$). Moreover, it is not possible to obtain data collapse according to the full scaling relation equation (7), with temperatures corresponding to $0.02 \lesssim \epsilon \lesssim 0.8$ (or to $0.25 \lesssim \epsilon \lesssim 0.8$), for any choice of $T_g$, $z\nu$ and $\beta$. Based on the estimates of $KV_m$ and $\tau_0$ for the dilute sample and the temperature range used in the analysis above, it is expected that $\tau_* \sim 10^{-9}$–$10^{-7}$ s. However, the derived value ($\tau_* \sim 10^{-4.6}$) deviates by orders of magnitude from this range. Furthermore, even with an Arrhenius–Néel temperature dependence of $\tau_*$, it is not possible to obtain unambiguous parameters from the critical slowing down analysis and to fulfil scaling according to equation (7). A simple manifestation of critical dynamics, which is independent of a temperature dependence of $\tau_*$, is that $\chi''(\omega)/\omega\chi_{eq}$ should settle on plateaus for small values of $\omega$. Referring to figure 7($a$), it is seen that this prediction is not fulfilled for the 5 vol% sample (except for $T \geqslant 65$ K), and this is a further indication of non-critical dynamics in this sample.

Several factors may contribute to deviations from critical behaviour and a possible non-divergence of the correlation length. First, there may be physical clustering of the particles (i.e., regions with a higher density of particles than average). The effect of clustering is twofold: at comparably high temperatures, where short-range correlations are relevant, the stronger inter-particle interaction in particle clusters will enhance the local correlation length and shift the dynamics to longer timescales than expected from the volume fraction of particles and a homogeneous particle dispersion. In addition, the small-scale heterogeneity will create a dispersion of length scales for the collective dynamics that modifies and possibly limits the growth of correlations at lower temperatures. Second, the polydispersivity of the particle

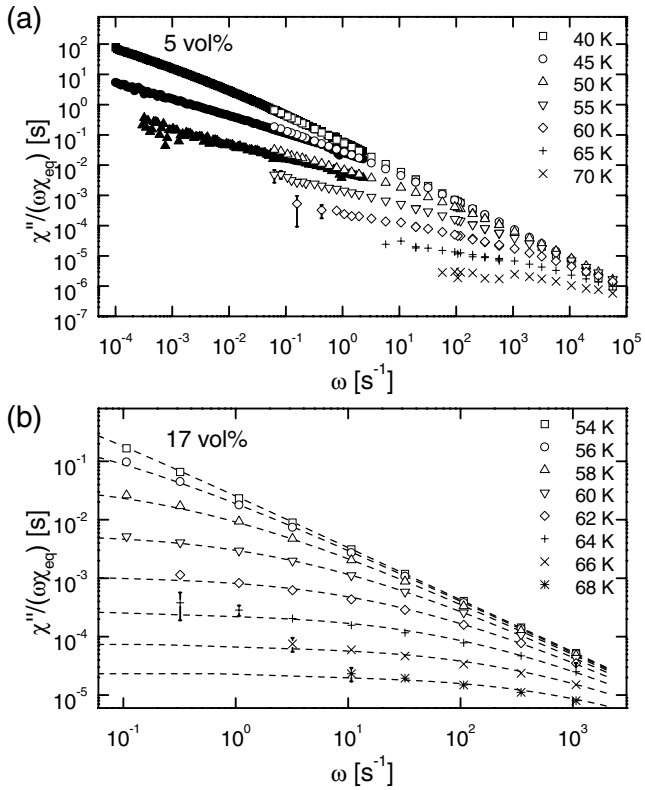


**Figure 8.** (*a*) A plot of the AC data (open points) and ZFC relaxation data (filled points) according to equation (8) for the 5 vol% sample. (*b*) A plot of the AC data according to equation (8) for the 17 vol% sample. The dashed curves are obtained from $G(x)$ with the expected asymptotic behaviours. Error bars are only shown when they are larger than the symbol size.

system leads to a distribution of single-particle relaxation times with a width that increases significantly with decreasing temperature (and is thus more important for the 5 vol% sample than for the 17 vol% sample). At lower temperatures, the largest particles may therefore become thermally blocked on timescales comparable to the longest timescale related to the collective dynamics and act as random magnets instead of taking part in the collective dynamics. This may completely mask or even obstruct long-range collective behaviour, as discussed in [11]. The non-critical behaviour of the present 5 vol% sample is most probably due both to the formation of clusters of particles (see section below) and to the dispersion of single-particle relaxation times.

### *3.3. Relaxation function*

For a spin glass and $T \lesssim T_g$, $S(T, t)$ is history dependent and has a non-trivial variation with $t$. However, when quasi-equilibrium is probed, one can write $S(T, t) \propto t^{-y(T)}$, where $y(T)$ attains a positive value close to zero [26]. For $T > T_g$, the time dependence of $S(T, t)$ is determined by the critical dynamics. As discussed previously, the critical dynamics results in fluctuations spanning all timescales between $\tau_*$ and $\tau_c$, and this gives a very broad spectrum of relaxation times. From equation (2) and using the asymptotic behaviours of $G(x)$ in

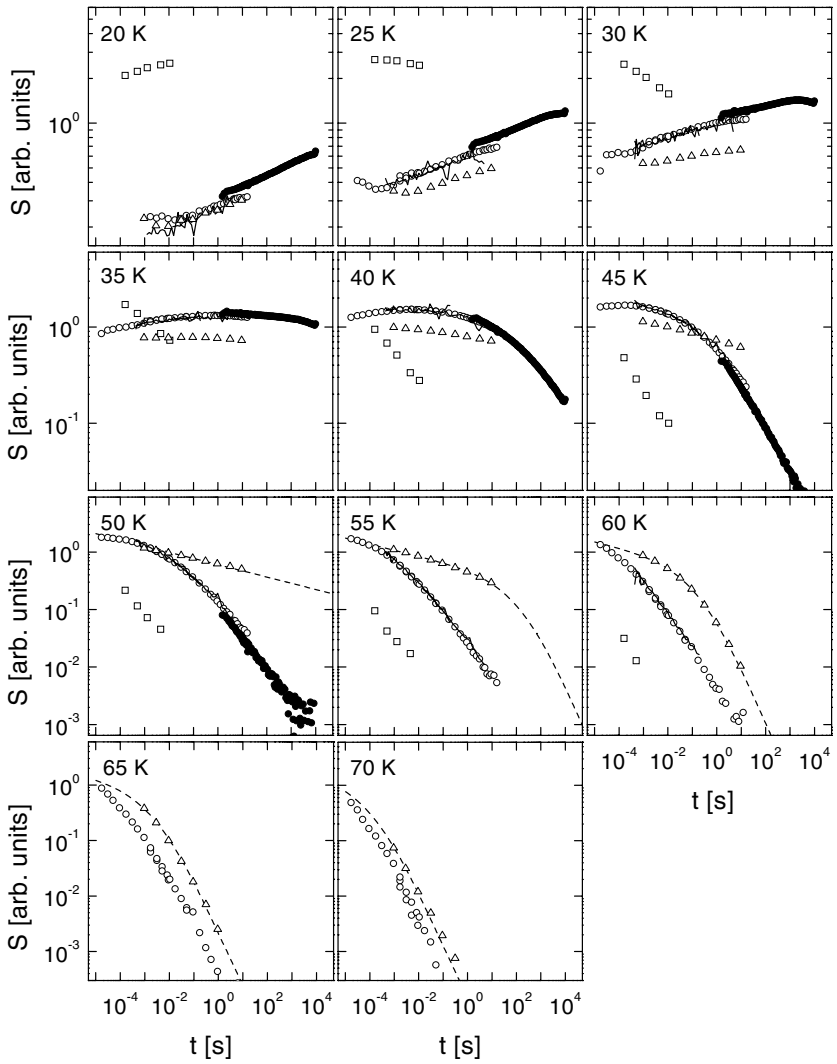


**Figure 9.** Relaxation rate versus observation time at different temperatures. For the 0.06 vol% sample (□) the relaxation rate is calculated from the AC susceptibility data. For the 5 vol% sample (○), the relaxation rate is calculated from AC susceptibility data (open symbols), ZFC data (filled symbols) and noise data (curves) and for the 17 vol% sample the relaxation rate is calculated from AC susceptibility data (△) and from $G(x)$ with the expected asymptotic behaviours (dashed curves).

equation (7), it is easily seen that $S(T, t) \propto t^{-y(T)}$ with $y(T) = \beta/z\nu \approx 0.1$ for $\tau_* \ll t \ll \tau_c$ and $y(T) = 1$ for $t \gg \tau_c$ [32]. At intermediate observation times, $y(T)$ monotonically increases with $t$ between the two extremes and a crossover (or 'knee') from an essentially flat $S(T, t)$ versus $t$ curve to $S(T, t) \propto t^{-1}$ is expected at $t \sim \tau_c$.

Figure 9 shows the relaxation rate versus time for the three samples at different temperatures in the range 20 K $\leqslant T \leqslant$ 70 K. For the 0.06 and 17 vol% samples, $\chi''$-data are shown, and for the 5 vol% sample, results from ZFC relaxation, AC susceptibility and magnetic noise measurements are included. For the 17 vol% sample, $\chi''$-data for $T > T_g$ obtained from equation (7) using the experimentally estimated $G(x)$ and the expected asymptotic behaviour for small $x$ are also shown. In the low-temperature region, $T \lesssim 30$ K, the magnitudes of the

relaxation rates for the two interacting samples are much smaller than that for the 0.06 vol% sample. This is a signature of collective dynamics [11, 33]. Moreover, the relaxation rate of the 17 vol% sample is smaller than that of the 5 vol% sample. For temperatures $T \gtrsim 40$ K and in the time window investigated, the relaxation rate of the 0.06 vol% sample decays with increasing observation time, while the relaxation rate of the 5 vol% sample at short timescales exhibits a weak frequency dependence followed by a knee and a decrease towards zero at longer timescales. This approach towards zero relaxation rate ($y(T) \approx 0.5$–$0.6$ between 45 and 55 K) is slower than that of an atomic spin glass (for which $y(T) = 1$) and consistent with the lack of plateaus in the $\chi''(\omega)/\omega\chi_{eq}$ curves for the corresponding temperatures in figure 8($a$). The time dependence of the relaxation rate at timescales below this knee is also uncharacteristic of a spin glass as it is non-monotonic in time and shows a broad maximum. For the 17 vol% sample and in the temperature range 35 K $\lesssim T \lesssim$ 50 K, the relaxation rate exhibits a slow, monotonic decrease with increasing observation time. The relaxation rate follows a $S(T, t) \propto t^{-y(T)}$ dependence, with $y(T)$ decreasing with decreasing temperature, mimicking the expected behaviour of a spin-glass system [26]. It should be noted though that the particle size distribution will cause a temperature-dependent and broad onset of the response on short observation times, as can be envisaged by the relaxation rate curves at the lowest temperatures. At temperatures above $T_g$, $T > 50$ K, a knee appears in the relaxation rate also for this sample and the approach towards zero follows $S(T, t) \propto t^{-1}$. At temperatures $T \geqslant 65$ K, the cut-off in the relaxation rate is equally sharp for both interacting samples, and the dynamics of the two samples are rather similar. This indicates, for the 5 vol% sample, that the particle moments participating in the dynamics on long timescales in this temperature range are more strongly interacting than average, i.e. that these particles are part of agglomerates showing properties similar to those of the 17 vol% sample.

## 4. Conclusions

Extensive studies of the magnetic dynamics of a nanoparticle system containing nearly monodisperse ferromagnetic particles have been presented. We have shown that a strongly interacting particle system (the 17 vol% sample) displays critical dynamics reminiscent of that of a spin glass. Furthermore, the effect of an Arrhenius–Néel temperature dependence of $\tau_*$ has been explored and it has been found that dynamic scaling for this sample prevails although with slightly reduced values of the critical exponents $z\nu$ and $\beta$. The values of $\tau_0$ and $KV_m$ obtained in this analysis are comparable to those found for the 0.6 vol.% sample, which is as expected as $\tau_*$ is related to the superparamagnetic relaxation time of a single particle, and the majority of the effect of the inter-particle interactions should be accounted for by the critical divergence, $(T/T_g - 1)^{-z\nu}$, in equation (5).

For weakly interacting particle systems, the dipolar interaction will only slightly modify the relaxation compared to a non-interacting system, and the relaxation time can be obtained by introducing thermodynamical averages of the dipolar field in an expression for the single-particle relaxation time, as suggested in [24]. Such a theory will apply for the most dilute sample studied here (the 0.06 vol% sample) near the blocking temperature.

For a wide range of particle concentrations (interaction strengths), neither a pure model for weakly interacting systems nor a model only assuming critical dynamics will correctly describe the magnetic relaxation of an interacting particle system. In the present work, this has been illustrated by the 5 vol% sample, in which correlations and collective behaviour are of importance, as evidenced by non-equilibrium dynamics similar to that exhibited by spin glasses [10] and an apparent critical slowing down in a limited temperature range. Yet, the deviation from critical slowing down at lower temperatures and the failure to satisfy other

signatures of critical dynamics show that the slowing down of the magnetic dynamics in this sample differs profoundly from that in spin glasses. The range of concentrations for which such a complex behaviour occurs becomes wider with increasing width of the particle size distribution, as can be evidenced by comparing to the system studied in [11]. For the sample used in that study, the relative dipole interaction strength ($=M_s^2\phi/K$) is comparable to that of the 17 vol% sample studied here, but that sample has a much wider energy barrier distribution and does not exhibit critical dynamics although it showed collective behaviour.

## Acknowledgment

This work was financially supported by The Swedish Natural Science Research Council (NFR). We would like to thank Christian Bender Koch for the atomic absorption spectroscopy measurements.

## References

[1] Luo W, Nagel S R, Rosenbaum T F and Rosensweig R E 1991 *Phys. Rev. Lett.* **67** 2721
[2] Mørup S 1994 *Europhys. Lett.* **28** 671
[3] Dormann J L, Fiorani D and Tronc E 1997 *Adv. Chem. Phys.* **98** 283
[4] Djurberg C, Svedlindh P, Nordblad P, Hansen M F, Bødker F and Mørup S 1997 *Phys. Rev. Lett.* **79** 5154
[5] Dormann J L, Cherkaoui R, Spinu L, Noguès M, Lucari F, D'Orazio F, Fiorani D, Garcia A, Tronc E and Jolivet J P 1998 *J. Magn. Magn. Mater.* **187** L139
[6] Jonsson T, Svedlindh P and Hansen M F 1998 *Phys. Rev. Lett.* **81** 3976
[7] Mamiya H, Nakatani I and Furubayashi T 1999 *Phys. Rev. Lett.* **82** 4332
[8] Hansen M F and Mørup S 1998 *J. Magn. Magn. Mater.* **184** 262
Dormann J L, Fiorani D and Tronc E 1999 *J. Magn. Magn. Mater.* **202** 251 and references therein
[9] Mamiya H and Nakatani I 1999 *Nanostruct. Mater.* **12** 859
[10] Jönsson P, Hansen M F and Nordblad P 2000 *Phys. Rev.* B **61** 1261
[11] Jonsson T, Nordblad P and Svedlindh P 1998 *Phys. Rev.* B **57** 497
[12] Wonterghem J V, Mørup S, Charles S W and Wells S 1998 *J. Colloid Interface Sci.* **121** 558
[13] Fisker R, Carstensen J M, Hansen M F, Bødker F and Mørup S 2000 *J. Nanoparticle Res.* **2** 267
[14] Hansen M F, Bødker F, Mørup S, Djurberg C and Svedlindh P 1998 *J. Magn. Magn. Mater.* **177–81** 928
[15] Magnusson J, Djurberg C, Granberg P and Nordblad P 1997 *Rev. Sci. Instrum.* **68** 3761
[16] Lundgren L, Svedlindh P and Beckman O 1981 *J. Magn. Magn. Mater.* **25** 33
[17] Callen H B and Welton T A 1951 *Phys. Rev.* **83** 34
[18] Raĭkher Y L and Stepanov V I 1997 *Phys. Rev.* B **55** 15 005
[19] Jonsson T, Mattsson J, Nordblad P and Svedlindh P 1997 *J. Magn. Magn. Mater.* **168** 269
[20] Hanson M, Johansson C and Mørup S 1993 *J. Phys.: Condens. Matter* **5** 725
[21] Hanson M, Johansson C, Pedersen M S and Mørup S 1995 *J. Phys.: Condens. Matter* **7** 9269
[22] Linderoth S, Balcells L, Labarta A, Tejada J, Henriksen P V and Sethi S A 1993 *J. Magn. Magn. Mater.* **124** 269
[23] García-Palacios J L 2000 *Adv. Chem. Phys.* **112** 1
[24] Jönsson P and García-Palacios J L 2001 *Europhys. Lett.* **55** 418
[25] Hohenberg P C and Halperin B I 1977 *Rev. Mod. Phys.* **49** 435
[26] Ogielski A T 1985 *Phys. Rev.* B **32** 7384
[27] Rigaux C 1995 *Ann. Phys., Paris* **20** 445
[28] Gunnarsson K, Svedlindh P, Nordblad P, Lundgren L, Aruga H and Ito A 1988 *Phys. Rev. Lett.* **61** 754
[29] Jönsson P, Svedlindh P, Nordblad P and Hansen M F 2001 *J. Magn. Magn. Mater.* **226** 1315
[30] Geschwind S, Huse D A and Devlin G E 1990 *Phys. Rev.* B **41** 2650
[31] Gunnarsson K, Svedlindh P, Nordblad P, Lundgren L, Aruga H and Ito A 1991 *Phys. Rev.* B **43** 8199
[32] Strictly, the limit stated for $\tau \gg \tau_c$ holds only for $S(T, t)$ derived from $\chi''$. For ZFC relaxation data, an exponential decay of $S(T, t)$ is expected for $t > \tau_c$, see
Lundgren L, Nordblad P and Svedlindh P 1986 *Phys. Rev.* B **34** 8164
[33] Andersson J-O, Djurberg C, Jonsson T, Svedlindh P and Nordblad P 1997 *Phys. Rev.* B **56** 13 983